

# Spring pendulum system

Jonas Grutter, Chloe Mondon

[jonas.grutter@epfl.ch](mailto:jonas.grutter@epfl.ch), [chloe.mondon@epfl.ch](mailto:chloe.mondon@epfl.ch)

August 17, 2021

## Contents

<b>1</b>	<b>Introduction</b>	<b>2</b>
<b>2</b>	<b>Analytical calculation</b>	<b>3</b>
2.1	Differential equation of motion . . . . .	3
2.2	Equilibrium position, $(x_{eq}, y_{eq})$ when $E_x = E_y = 0$ and $\nu = 0$ . . . . .	4
2.2.1	Equilibrium position stability analysis . . . . .	5
2.3	Expression of mechanical energy, $E_{mec}$ . . . . .	6
2.4	Power of non-conservative forces, $P_{nc}$ . . . . .	6
2.5	Natural frequency of the system : $\omega_1, \omega_2$ . . . . .	6
<b>3</b>	<b>Numerical simulations</b>	<b>8</b>
3.1	Small movements around the stable equilibrium position (5) ( $E_x = E_y = 0; \nu = 0$ ) . . . . .	8
3.1.1	Analytical solutions . . . . .	8
3.1.2	Comparaison between the analytical and numerical solution . . . . .	9
3.1.3	Convergence rate . . . . .	10
3.2	Resonant excitation . . . . .	12
3.2.1	Vertical excitation: $E_x = 0 \frac{\text{V}}{\text{m}}, E_y = 1 \frac{\text{V}}{\text{m}}, \omega = \omega_1$ . . . . .	12
3.2.2	Horizontal excitation: $E_x = 1 \frac{\text{V}}{\text{m}}, E_y = 0 \frac{\text{V}}{\text{m}}, \omega = \omega_2$ . . . . .	14
3.3	Big movement without depreciation and without excitation . . . . .	16
3.3.1	Simulation by varying $0 < \delta \leq 5m$ . . . . .	17
3.3.2	Study on the conservation of $E_{mec}$ when $\delta = 3$ and convergence rate . . . . .	18

3.4	Big movement without depreciation, with excitation . . . . .	20
3.4.1	Theorem of mechanical energy . . . . .	20
3.4.2	Poincaré section . . . . .	21
3.4.3	Sensitivity to initial conditions . . . . .	23
3.5	Big movement with damping and with excitation . . . . .	27
3.5.1	Verification of the Mechanical Energy Theorem . . . . .	27
3.5.2	Signature of chaos : sensitivity to initial condition . . .	28
3.5.3	The Poincaré section . . . . .	29
3.5.4	Strange attractor . . . . .	31
<b>4</b>	<b>Optional</b>	<b>33</b>
4.1	Inclusion of an oscillating force resulting from the application of torque . . . . .	33
<b>5</b>	<b>Conclusion</b>	<b>35</b>

# 1 Introduction

The main purpose of this exercise is to introduce the notion of chaos and to observe the difference between a stable and chaotic system. The chaos is characterised by a major sensitivity to the initial conditions. Two new notions are used : the Verlet scheme and the Poincaré section. The Verlet Scheme is obtained by dividing the time step  $\Delta t$  by two. For the first half, the Euler-Cromer algorithm is used. For the second half, the Euler-Cromer algorithm is also used, but in an other way (it is possible to use Euler-Cromer in two different ways, see [1] page 31). It is important to note that the theoretical convergence rate of the Verlet scheme is two [1]. The definition of the Poincaré section is given in section 3.4.2.

In this study, one is looking at the motion of a spring pendulum, of which a mass is attached to its extremity. First, one is interested in the small movements around the stable equilibrium position. These movements are studied by very slightly disturbing the stable equilibrium position on the x-axis then on the y-axis. Then, simulations around the stable equilibrium position are studied with vertical and horizontal excitation. Next, large movements without damping or excitation are studied. In order to do this, the pendulum must be moved much further away from its equilibrium position than in the first simulation. After that, large movements without damping and

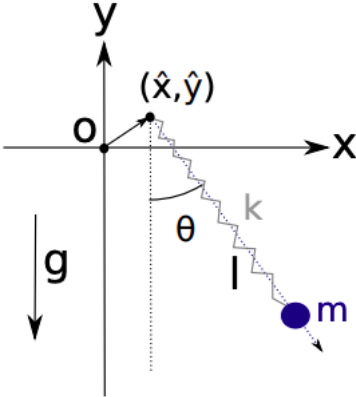


Figure (1) Mechanism of the spring pendulum

with excitation are analyzed. Moreover, the theorem of mechanical energy is checked, Poincaré sections are plotted and sensitivity to the initial conditions is studied. To continue, the large movements of the pendulum with damping and excitation are studied. The same points as in the previous simulation are analyzed. In this case, another concept can be analyzed, that of strange attractor. Finally, as an optional point, an oscillating force resulting from the application of torque is applied.

## 2 Analytical calculation

### 2.1 Differential equation of motion

In this section, the differential equations that describe the movement of a spring pendulum are computed. Four forces act on the pendulum:  $\mathbf{P}$  the force of gravitation,  $\mathbf{F}_k$  the force of spring,  $\mathbf{F}_E$  an oscillating excitation force and  $\mathbf{F}_T$  the frictional force. Using the cartesian coordinates,  $L = \sqrt{x^2 + y^2}$ ,  $\cos(\theta) = -\frac{y}{\sqrt{x^2+y^2}}$  and  $\sin(\theta) = \frac{x}{\sqrt{x^2+y^2}}$ , the projection of the forces is :

- $\mathbf{P} = -m \cdot g \mathbf{e}_y$
- $\mathbf{F}_k = -k \cdot (L - l_0) \mathbf{e}_L = -k \cdot (\sqrt{x^2 + y^2} - l_0) \cdot \left( \frac{x}{\sqrt{x^2+y^2}} \mathbf{e}_x + \frac{y}{\sqrt{x^2+y^2}} \mathbf{e}_y \right)$
- $\mathbf{F}_E = q \cdot (E_x \cdot \cos(\omega t) \mathbf{e}_x + E_y \cdot \cos(\omega t) \mathbf{e}_y)$

- $\mathbf{F}_T = \mathbf{v} \cdot \nu$

Using Newton's law,  $\sum \mathbf{F} = m\mathbf{a}$ , we get two differential equations according to the cartesian axes:

$$\begin{cases} \ddot{x} = \frac{1}{m} \cdot (-k \cdot (\sqrt{x^2 + y^2} - l_0) \cdot \frac{x}{\sqrt{x^2+y^2}} + q \cdot E_x \cos(\omega t) - \nu \cdot v_x) \\ \ddot{y} = \frac{1}{m} \cdot (-k \cdot (\sqrt{x^2 + y^2} - l_0) \cdot \frac{y}{\sqrt{x^2+y^2}} + q \cdot E_y \cdot \cos(\omega t) + \nu \cdot v_y) - g \end{cases} \quad (1)$$

## 2.2 Equilibrium position, $(x_{eq}, y_{eq})$ when $E_x = E_y = 0$ and $\nu = 0$

With the hypothesis that  $E_x = E_y = 0$  and  $\nu = 0$ , the system can be rewritten as :

$$\begin{cases} \ddot{x} = -\frac{k}{m} \cdot (\sqrt{x^2 + y^2} - l_0) \cdot \frac{x}{\sqrt{x^2+y^2}} \\ \ddot{y} = -\frac{k}{m} \cdot (\sqrt{x^2 + y^2} - l_0) \cdot \frac{y}{\sqrt{x^2+y^2}} - g \end{cases}$$

The system is at equilibrium when  $\ddot{x} = \ddot{y} = 0$ . Imposing these conditions, the equilibrium positions are found.

$$\begin{cases} 0 = -\frac{k}{m} \cdot (\sqrt{x_{eq}^2 + y_{eq}^2} - l_0) \cdot \frac{x_{eq}}{\sqrt{x_{eq}^2+y_{eq}^2}} \\ 0 = -\frac{k}{m} \cdot (\sqrt{x_{eq}^2 + y_{eq}^2} - l_0) \cdot \frac{y_{eq}}{\sqrt{x_{eq}^2+y_{eq}^2}} - g \end{cases}$$

On the x-axis,  $\frac{k}{m\sqrt{x_{eq}^2+y_{eq}^2}} \neq 0$  because all parameters are non-zero constants.

This implies that  $\sqrt{x_{eq}^2 + y_{eq}^2} - l_0 = 0$  or  $x_{eq} = 0$ .

Let's consider the first case, inserting the condition  $\sqrt{x_{eq}^2 + y_{eq}^2} - l_0 = 0$  in the second differential equation we get :

$$0 = -\frac{k}{m} \cdot 0 \cdot \frac{y_{eq}}{\sqrt{x_{eq}^2 + y_{eq}^2}} - g \Leftrightarrow g = 0 \quad (2)$$

Since  $g = 9.81\text{ms}^{-1}$ , this is absurd. Hence,  $x_{eq} = 0$ . Inserting  $x_{eq} = 0$  in the second differential equation enables to find  $y_{eq}$ .

$$y_{eq} = -\frac{gm}{k} \pm l_0 \quad (3)$$

Thus, there are two equilibrium position  $(0, -\frac{gm}{k} - l_0)$  and  $(0, -\frac{gm}{k} + l_0)$ .

### 2.2.1 Equilibrium position stability analysis

In order to determine which position is stable, one have to calculate the derivatives of the potential energy. Hence, one can compute its Hessian matrix. If the determinant is positive the position is stable.

- $\frac{\partial^2 E_{pot}}{\partial x^2} = k - kl_0((x^2 + y^2)^{-\frac{1}{2}} - x^2(x^2 + y^2)^{-\frac{3}{2}})$
- $\frac{\partial^2 E_{pot}}{\partial y^2} = k - kl_0((x^2 + y^2)^{-\frac{1}{2}} - y^2(x^2 + y^2)^{-\frac{3}{2}})$
- $\frac{\partial^2 E_{pot}}{\partial x \partial y} = kxyl_0 \cdot (x^2 + y^2)^{-\frac{3}{2}}$

The Hessian matrix at the equilibrium position is given by :

$$Hess(E_{mec})(x_{eq}, y_{eq}) = \begin{pmatrix} \frac{\partial^2 E_{pot}}{\partial x^2} & \frac{\partial^2 E_{pot}}{\partial x \partial y} \\ \frac{\partial^2 E_{pot}}{\partial x \partial y} & \frac{\partial^2 E_{pot}}{\partial y^2} \end{pmatrix} (x_{eq}, y_{eq}) = k \begin{pmatrix} 1 - \frac{l_0}{|y_{eq}|} & 0 \\ 0 & 1 \end{pmatrix} \quad (4)$$

For  $(x_{eq}, y_{eq}) = (0, -\frac{gm}{k} - l_0)$ , the determinant of the matrix is:

$$\det(Hess(E_{mec})(0, -\frac{gm}{k} - l_0)) \simeq 0.74 > 0 \quad (5)$$

Hence, the position  $(x_{eq}, y_{eq}) = (0, -\frac{gm}{k} - l_0)$  is stable.

For the other analytical equilibrium position  $(x_{eq}, y_{eq}) = (0, -\frac{gm}{k} + l_0)$ , even if we have:

$$\det(Hess(E_{mec})(0, -\frac{gm}{k} + l_0)) \simeq 0.49 > 0 \quad (6)$$

This position is not a stable equilibrium position because this position is not physically possible (because of the value of the parameters  $l_0$ ,  $k$ ,  $g$  and  $m$  given in this problem). This means that it is not even a position that the pendulum can reach.

In the rest of the report, the equilibrium position will therefore be  $(x_{eq}, y_{eq}) = (0, -\frac{gm}{k} - l_0)$ .

## 2.3 Expression of mechanical energy, $E_{mec}$

Mechanical energy is expressed as :

$$E_{mec} = E_{kin} + E_{pot} \quad (7)$$

where  $E_{pot}$  is the sum of the potential gravitational energy  $E_g = mgy$  and the potential of the string  $E_k = \frac{1}{2}k(\sqrt{x^2 + y^2} - l_0)^2$ . So

$$E_{mec} = \frac{1}{2}m\mathbf{v}^2 + mgy + \frac{1}{2}k(\sqrt{x^2 + y^2} - l_0)^2 \quad (8)$$

where  $\mathbf{v}^2 = v_x^2 + v_y^2$ .

## 2.4 Power of non-conservative forces, $P_{nc}$

Non-conservative forces are dissipating forces such as friction or air resistance. These forces take energy away from the system as the system progresses, energy that you can not get back. These forces are path dependent; therefore it matters where the object starts and stops[2].

In this exercise, there are two dissipating forces:  $\mathbf{F}_E$  and  $\mathbf{F}_T$ . The power of a force is given by  $P = \mathbf{F} \cdot \mathbf{v}$  where  $v$  is the velocity of the object.

$$P_{nc} = \mathbf{F}_E \cdot \mathbf{v} + \mathbf{F}_T \cdot \mathbf{v} \quad (9)$$

## 2.5 Natural frequency of the system : $\omega_1, \omega_2$

In order to find the two natural frequencies of the system, the equation found in 2.1 is resolved under the approximation that the pendulum undergoes small movements around the stable equilibrium position (5) ( $E_x = E_y = 0; \nu = 0$ ). First, let's consider the case where the pendulum makes small movements only according to the horizontal axis x. Since the pendulum makes small movements, one can place the approximation that  $x = x_{eq} + \delta x$  and  $y = y_{eq}$ . Since  $x_{eq}$  is a constant there is the following relation :

$$\ddot{x} = (x_{eq} + \delta x)'' = \delta \ddot{x} \quad (10)$$

Using (5) :

$$\ddot{x} = \delta \ddot{x} = -\frac{k}{m} \cdot \frac{(\sqrt{(x_{eq} + \delta x)^2 + y_{eq}^2} - l_0)}{\sqrt{(x_{eq} + \delta x)^2 + y_{eq}^2}} \cdot \delta x = -\frac{k}{m} \cdot \frac{(\sqrt{\delta x^2 + y_{eq}^2} - l_0)}{\sqrt{\delta x^2 + y_{eq}^2}} \cdot \delta x \quad (11)$$

Terms in  $\delta x^2$  can be neglected and  $y_{eq}$  is replaced by its value found in (5).

$$\ddot{x} = \delta\ddot{x} = -\frac{g}{\frac{mg}{k} + l_0}\delta x = -\frac{g}{L_{eq}}\delta x \quad (12)$$

In order to simplify the notation let us assume that  $L_{eq} = \frac{mg}{k} + l_0$  where  $L_{eq}$  is the length of the spring at equilibrium.

It is a differential equation of a harmonic oscillator. The solution of this type equation is given by  $\delta x = A\cos(\omega t) + B\sin(\omega t)$ , where A and B are the amplitude, t the time and  $\omega$  the frequency.

$$\delta\ddot{x} = -\omega^2 A\cos(\omega t) - \omega^2 B\sin(\omega t) = -\frac{g}{L_{eq}}(A\cos(\omega t) + B\sin(\omega t)) \Leftrightarrow \omega = \omega_2 = \sqrt{\frac{g}{L_{eq}}} \quad (13)$$

Secondly, let's consider the case where the pendulum makes small movements only according to the vertical axis y. For the same reason of above  $y = y_{eq} + \delta y$  and

$$\ddot{y} = (y_{eq} + \delta y)'' = \delta\ddot{y} \quad (14)$$

The differential equation is given by :

$$\ddot{y} = \delta\ddot{y} = -\frac{k}{m} \frac{(\sqrt{x_{eq}^2 + (y_{eq} + \delta y)^2} - l_0)}{\sqrt{x_{eq}^2 + (y_{eq} + \delta y)^2}} \cdot (y_{eq} + \delta y) - g = -\frac{k}{m} \frac{\sqrt{(1 + \frac{\delta y}{y_{eq}})^2} - l_0}{\sqrt{1 + (\frac{\delta y}{y_{eq}})^2}} \cdot (y_{eq} + \delta y) - g \quad (15)$$

Terms in  $\delta y^2$  can be neglected :

$$\delta\ddot{y} = -\frac{k}{m} \frac{\sqrt{1 + 2\frac{\delta y}{y_{eq}}} - l_0}{\sqrt{1 + 2\frac{\delta y}{y_{eq}}}} \cdot (y_{eq} + \delta y) - g \quad (16)$$

The first degree limited development of  $\sqrt{1+x} = 1 + \frac{x}{2} + O(x^2)$ . Hence,

$$\delta\ddot{y} = -\frac{k}{m} (y_{eq} + \delta y - l_0) \left( \frac{y_{eq} + \delta y}{y_{eq} + \delta y} \right) - g = -\frac{k}{m} \left( \frac{-mg}{k} + l_0 + \delta y - l_0 \right) - g = -\frac{k}{m} \delta y \quad (17)$$

It is also a differential equation of a harmonic oscillator.

$$\delta\ddot{y} = -\omega^2 A\cos(\omega t) - \omega^2 B\sin(\omega t) = -\frac{k}{m}(A\cos(\omega t) + B\sin(\omega t)) \Leftrightarrow \omega = \omega_1 = \sqrt{\frac{k}{m}} \quad (18)$$

### 3 Numerical simulations

#### 3.1 Small movements around the stable equilibrium position (5) ( $E_x = E_y = 0; \nu = 0$ )

In this section, the goal is to simulate small movements around the stable equilibrium position in two different cases : at the position  $(x_{eq} + \delta, y_{eq})$  and than at  $(x_{eq}, y_{eq} + \delta)$ . In both situation, the simulation is done on 5 periods using  $\Delta t = 0.05$ s. The analytical and numerical solutions are compared and a convergence rate study on  $\Delta t$  is done in order to determine the convergence rate of the Verlet scheme.

##### 3.1.1 Analytical solutions

In order to compare the analytical solution with the numerical one. The analytical solutions are calculated by solving the differential equation using the initial condition.

**Initial position :**  $(x_{eq} + \delta, y_{eq})$

At time  $t = 0$ , the solution is :

$$\delta x = x_0 = 10^{-6} = A \cos(\omega_2 t) + B \sin(\omega_2 t) \Leftrightarrow A = 10^{-6}$$

$\dot{\delta x} = 0 = -A \sin(\omega_2 t) + B \cos(\omega_2 t) \Leftrightarrow B = 0$  Which implies (for all  $t$ ) :

$$x_{th} = 10^{-6} \cos(\omega_2 t) \quad (19)$$

Hence, at  $t_{f2} = 5 \cdot \frac{2\pi}{\omega_2} \simeq 20.98$ s (time for a simulation of  $T = 5$ ):

$$x_{th} = 10^{-6} \text{m} \quad (20)$$

where  $x_{th}$  is the theoretical position on x at  $t_{f2}$ .

**Initial position :**  $(x_{eq}, y_{eq} + \delta)$

By proceeding exactly the same way as above one get for all  $t$  :

$$y_{th} = -4.37 + 10^{-6} \cos(\omega_1 t) \quad (21)$$

Hence, at  $t_{f1} = 5 \cdot \frac{2\pi}{\omega_1} \simeq 18.14$ s :

$$y_{th} = y_{eq} + \delta = -4.369999 \text{m} \quad (22)$$

where  $y_{th}$  is the theoretical position on y.

### 3.1.2 Comparaison between the analytical and numerical solution

To begin, one looks at the small movements around the position  $(x_{eq} + \delta, y_{eq})$ . In this part,  $\Delta t = 0.005$  s As one can see on Fig.2 the pendulum position in x oscillates between  $\simeq 10^{-6}$ m and  $-10^{-6}$ m. The pendulum position in y remains constant (The very small oscillations are due to rounding errors). Indeed, looking at Fig.4 it can be seen that  $v_y = 0$ . The error between the analytical and the numerical solution at  $t_{f1}$  for y is  $\approx 6.4 \cdot 10^{-12}$ . With regards to the small movements around the position  $(x_{eq}, y_{eq} + \delta)$ . One can notice that it is exactly the opposite of above. Indeed, Fig.3 shows that the position in y oscillates between  $\simeq -4.369999$ m and  $-4.37001$ m and that the position in x remains constant which is illustrated by the Fig.4. As expected  $v_x = 0$ . The error between the analytical and the numerical solution at  $t_{f2}$  for x is given by  $error = 4.9 \cdot 10^{-12}$ .

In both cases the error is minimal and it can be associated to rounding errors. It proves that Verlet methods is very good.

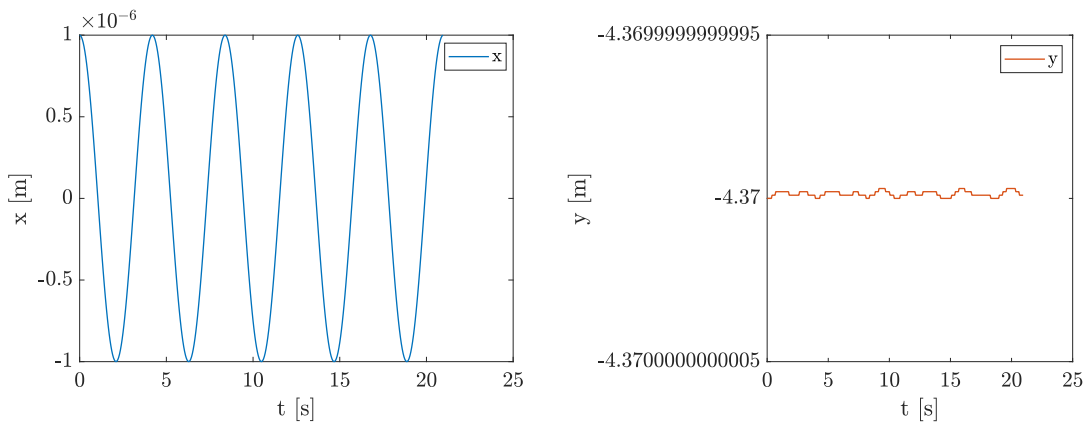


Figure (2) Small movements around the position  $(x_{eq} + \delta, y_{eq})$  over 5 period,  $t_f = t_{f2}$ .

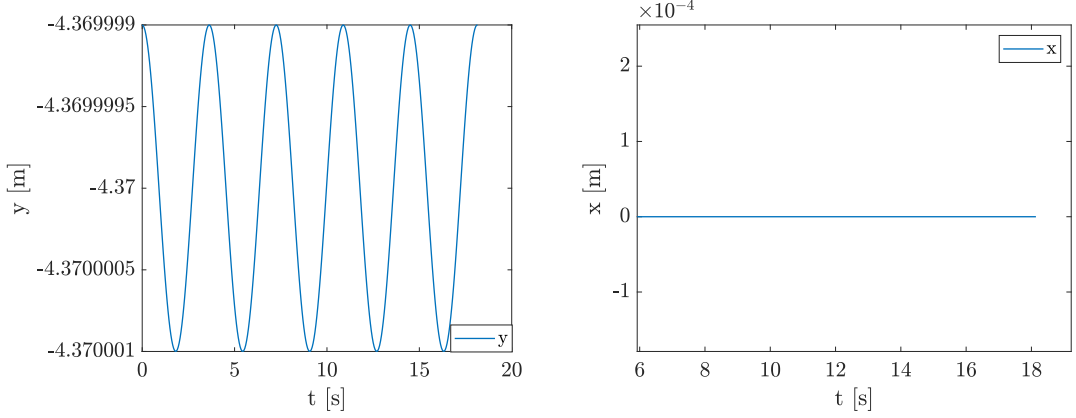


Figure (3) Small movements around the position  $(x_{eq}, y_{eq} + \delta)$  over 5 period,  $t_f = t_{f1}$ .

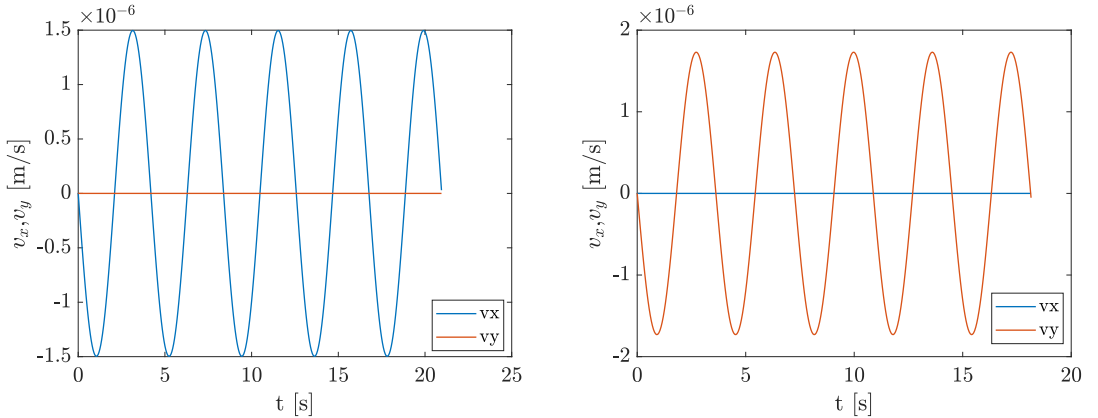


Figure (4) Velocity of the small movement during 5 periods. Left:  $(x_0, y_0) = (x_{eq} + \delta, y_{eq})$ ,  $t_f = t_{f2}$ . Right:  $(x_0, y_0) = (x_{eq}, y_{eq} + \delta)$ ,  $t_f = t_{f1}$ .

### 3.1.3 Convergence rate

In this case, the analytical solutions for  $x$  and  $y$  at the final time are known, so it is possible to compute  $Error_x = x_{Analytical} - x_{Numerical}$ ,  $Error_y = y_{Analytical} - y_{Numerical}$ . In a graphic which represents the error as a function of  $\Delta t$  with a log-log scale, the slope represents the convergence rate. So the linear fit of each curve in Fig 5 (which is represented by Fig 6) gives that the convergence rate is 2 for the Verlet method, which is the result predicted in the theory. In this case, the maximum of the error time was taken at all time.

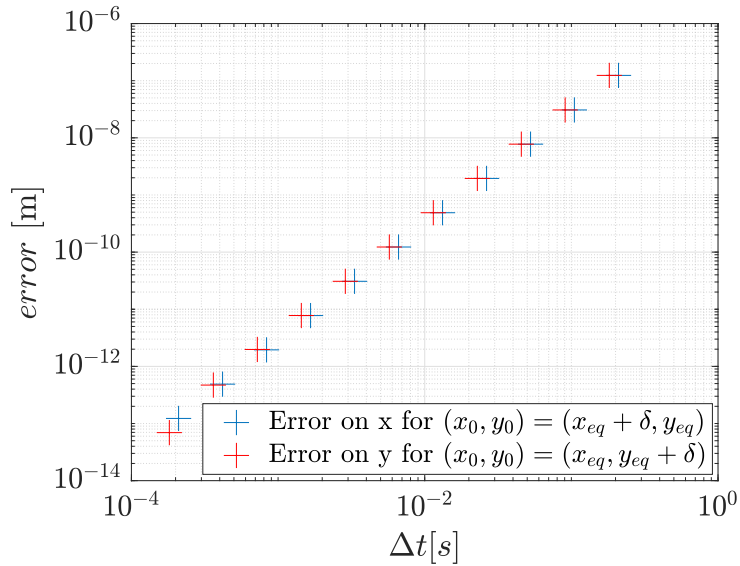


Figure (5) Convergence rate of the Verlet schemes for 11 simulations with a log-log scale

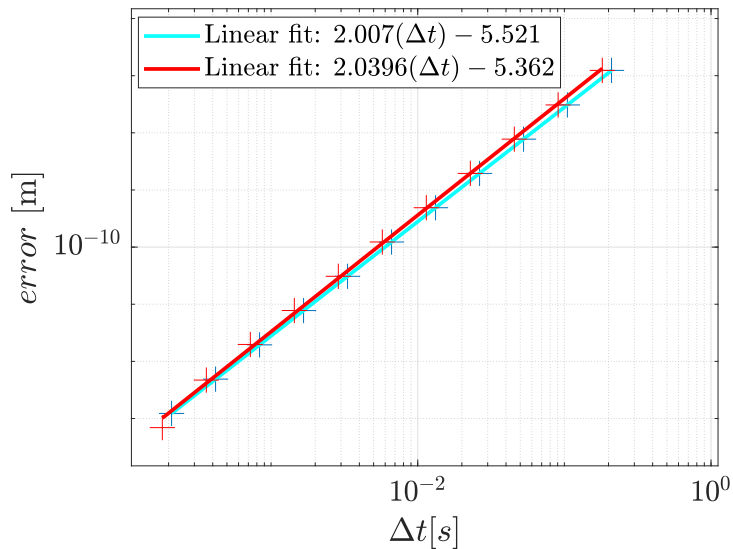


Figure (6) Convergence rate of the Verlet schemes for 11 simulations with a log-log scale with the fitting curve

### 3.2 Resonant excitation

In this section, the movement of the pendulum is analyzed when an electric field is applied.

Firstly, a vertical electric field is applied (Section 3.2.1). So  $E_x = 0 \frac{\text{V}}{\text{m}}$ ,  $E_y = 1 \frac{\text{V}}{\text{m}}$ . The frequency used in this case is  $\omega = \omega_1$ . Secondly, the electric field is horizontal (Section 3.2.2). So  $E_x = 1 \frac{\text{V}}{\text{m}}$ ,  $E_y = 0 \frac{\text{V}}{\text{m}}$  and  $\omega = \omega_2$ .

For both cases, the friction coefficient  $\nu = 0$  and the final time is  $t_{final} = 1000\text{s}$  (for almost all the simulations) and the initial position of the pendulum is its equilibrium position.

#### 3.2.1 Vertical excitation: $E_x = 0 \frac{\text{V}}{\text{m}}$ , $E_y = 1 \frac{\text{V}}{\text{m}}$ , $\omega = \omega_1$

Concerning mechanical energy when a vertical electric field is applied, it is possible to see that increases strongly over time (Fig 7 left). However, it does not diverge. Indeed, a longer simulation was carried out (Fig 7 right). This last one allows to conclude that the energy oscillates over time. The fact that the energy increases strongly is due to the fact that the frequency used is a proper frequency of the system.

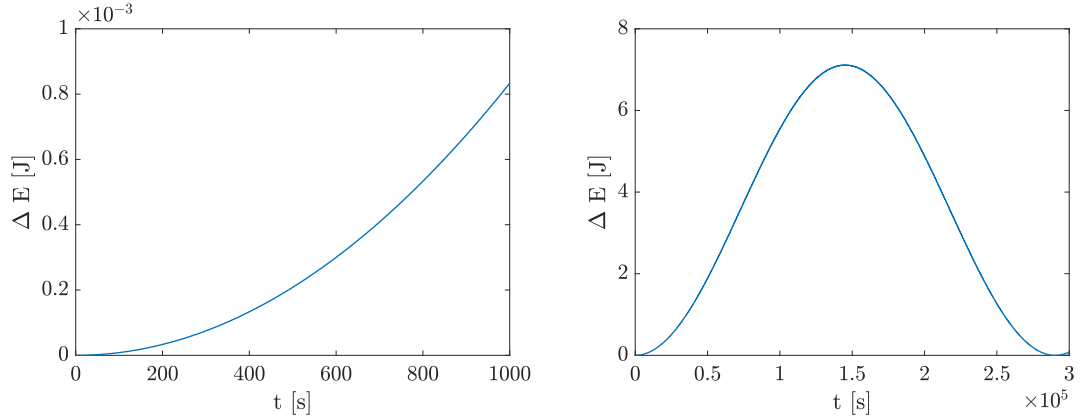


Figure (7) Energy as a function of the time in the case of a vertical excitation. Left:  $t_{final} = 1000\text{s}$ ,  $\Delta t = 0.001\text{s}$ . Right:  $t_{final} = 300000\text{s}$ ,  $\Delta t = 0.01\text{s}$

In order to see why the energy increases strongly over time, the trajectory and the velocity of the pendulum were studied Fig 8. These graphs show that the position in x remains constant ( $v_x$  remains 0 in the right side and  $x_0 = 0$ )

and that the position in  $y$  oscillates very fast more and more highly (Fig 8). That means that the velocity increases over the time. Indeed, Fig 8(left) shows this fact. That means that the kinetic energy increases more and more over the time. That is why the mechanical energy increases strongly. With a far longer simulation, it is possible to see that the velocity Speed does not grow infinitely, but it does oscillate (that is why the mechanical energy oscillate).

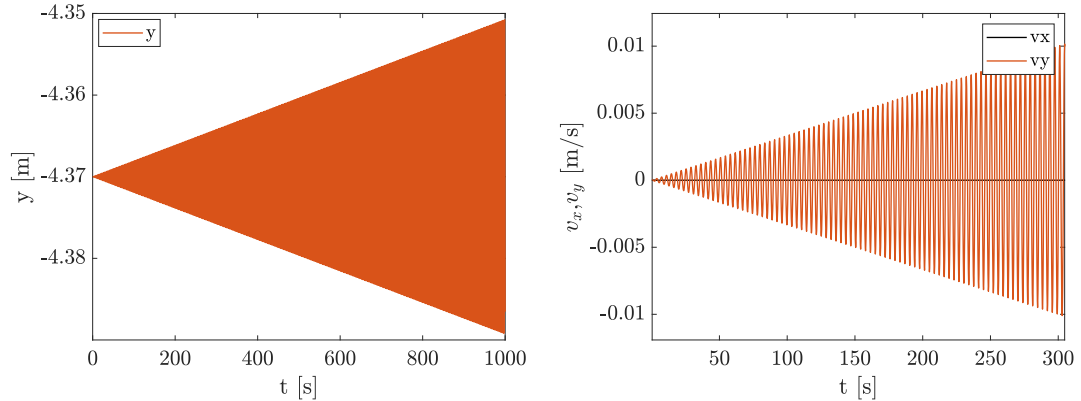


Figure (8) Left: Position of the pendulum as a function of the time in the case of a vertical excitation. Right: Velocity of the pendulum as a function of the time in the case of a vertical excitation (zoomed). Parameters used:  $t_{final} = 1000$  s,  $\Delta t = 0.001$  s.

In order to check why the mechanical energy increases strongly when the frequency is a proper frequency. The maximum energy  $E_{max}$  is plotted as a function of  $\omega$  for a frequency range close to  $\omega_1$  (Fig 9). This graph immediately highlights the jump in the mechanical energy of the system around the proper frequency  $\omega_1$ .

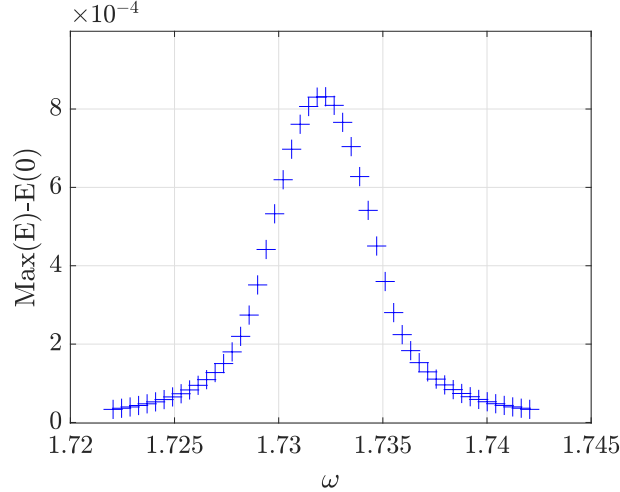


Figure (9) Energy as a function of the frequency  $\omega$  in the case of a horizontal excitation where the  $\omega$  are chosen near the second proper frequency  $\omega_1$

### 3.2.2 Horizontal excitation: $E_x = 1 \frac{\text{V}}{\text{m}}$ , $E_y = 0 \frac{\text{V}}{\text{m}}$ , $\omega = \omega_2$

In this section, the analyses are done in the same way as in the previous section 3.2.1. Concerning the energy, the results are very similar to the previous one. As it is possible to see on Fig 10 (right), the energy increases strongly when the frequency used is the other proper frequency of the system ( $\omega_2$ ) but it does not diverge (Fig. 10 right).

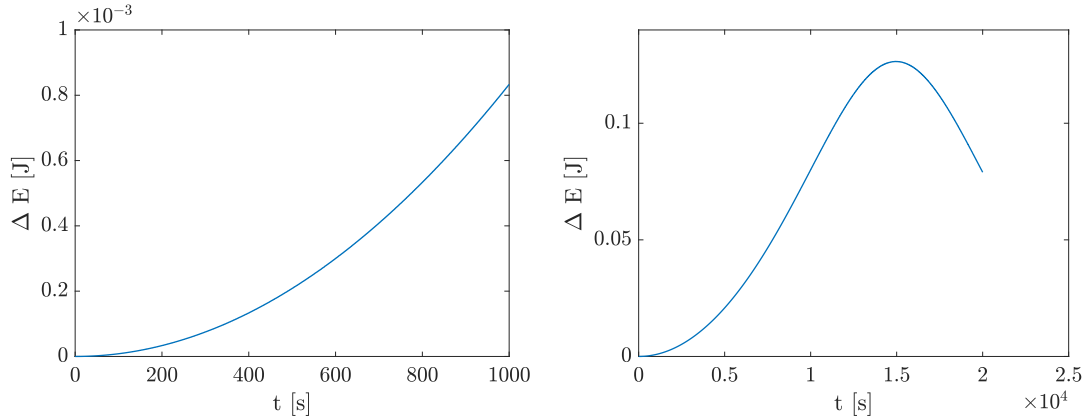


Figure (10) Energy as a function of the time in the case of a horizontal excitation. Left:  $t_{final} = 1000$ s,  $\Delta t = 0.001$  s. Right:  $t_{final} = 20000$  s,  $\Delta t = 0.001$  s

As it was done before, the trajectory and the velocity of the pendulum are plotted (Fig. 11). Here, it is possible to see that the position  $y$  remains constant and the position  $x$  oscillates very fast more and more highly as well as the velocity  $v_x$ . That is why the kinetic energy increases highly and so the mechanical energy increases too. As it was said before, the velocity does not grow infinitely but it does oscillate (with a far longer simulation).

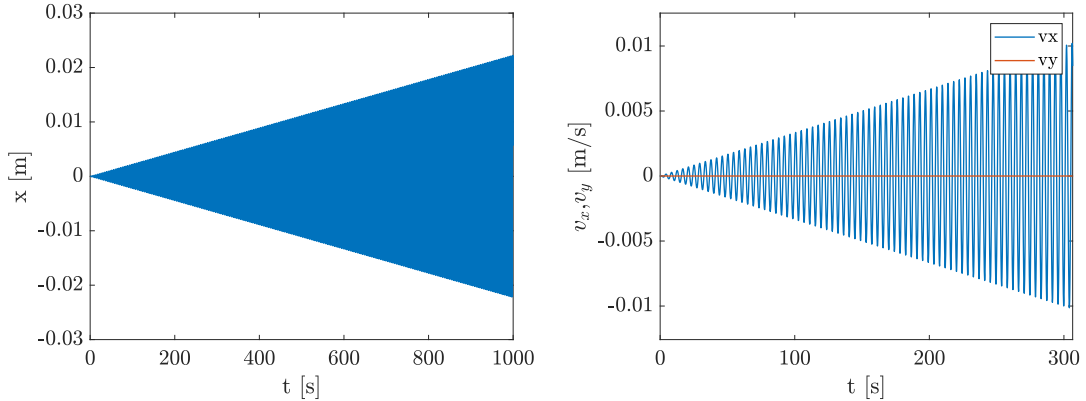


Figure (11) Left: Position of the pendulum as a function of the time in the case of a horizontal excitation. Right: Velocity of the pendulum as a function of the time in the case of a horizontal excitation (zoomed). Parameters used:  $t_{final} = 1000$ s,  $\Delta t = 0.001$  s.

Again, in order to check why the mechanical energy increases strongly when the frequency is the other proper frequency. The maximum energy  $E_{max}$  is plotted as a function of  $\omega$  for a frequency range close to  $\omega_2$  (Fig 12). Again, this graph immediately highlights the jump in the mechanical energy of the system around the second proper frequency  $\omega_2$ .

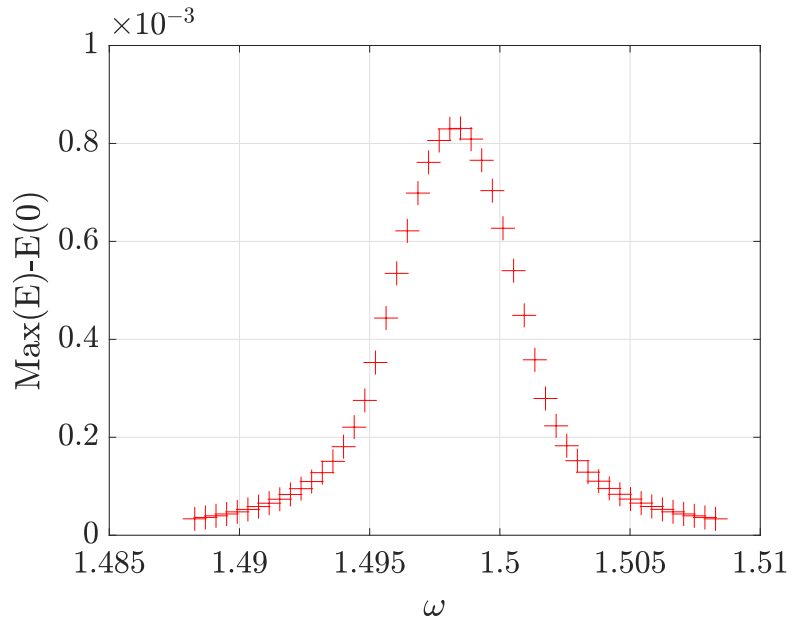


Figure (12) Energy as a function of the frequency  $\omega$  in the case of a horizontal excitation where the  $\omega$  are chosen near the second proper frequency  $\omega_2$ .

### 3.3 Big movement without depreciation and without excitation

In this section, the goal is to perform some simulations by varying  $0 < \delta \leq 5\text{m}$  and to study orbits in the planes  $(x, y)$ ,  $(x, v_x)$ ,  $(y, v_y)$  and  $(v_x, v_y)$ . The final time taken is  $t_f = 200\text{s}$  and  $\Delta t = 0.01\text{s}$ . The initial position used are  $x_0 = x_{eq} + \delta$  and  $y_0 = y_{eq} + \delta$ . The different values of  $\delta$  used are  $\delta = 1, 2, 3$  and  $5\text{m}$ . Then in the case where  $\delta = 3$  the conservation of  $E_{mec}$  is studied.

### 3.3.1 Simulation by varying $0 < \delta \leq 5m$

Observing Fig.13 one can notice that although the trajectory of the pendulum is complex it remains very regular and it fits into a certain geometric area very well defined. This is normal, since the pendulum does not experience any friction or excitation. The trajectory is therefore determined only from the initial conditions. Thanks to the superposition of the orbits the difference in their size can be observed. The more  $\delta$  is increased the wider is the trajectory of the pendulum. Even in the situation where the initial position is far away from the equilibrium position ( $\delta = 5m$ ), the behaviour of the pendulum remains regular and non-chaotic.

Exactly the same remarks can be made for the velocity graph (Fig.14). when  $\delta = 5$  the velocity is approximately 5 times bigger than when  $\delta = 1$ , 3 times bigger than when  $\delta = 2$  and 2 times bigger than when  $\delta = 3$ .

Fig.15 shows that the orbits in the planes  $(x, v_x)$  and  $(y, v_y)$  are practically identical. It represents an ellipse. This explains the symmetry one can see on Fig.14.

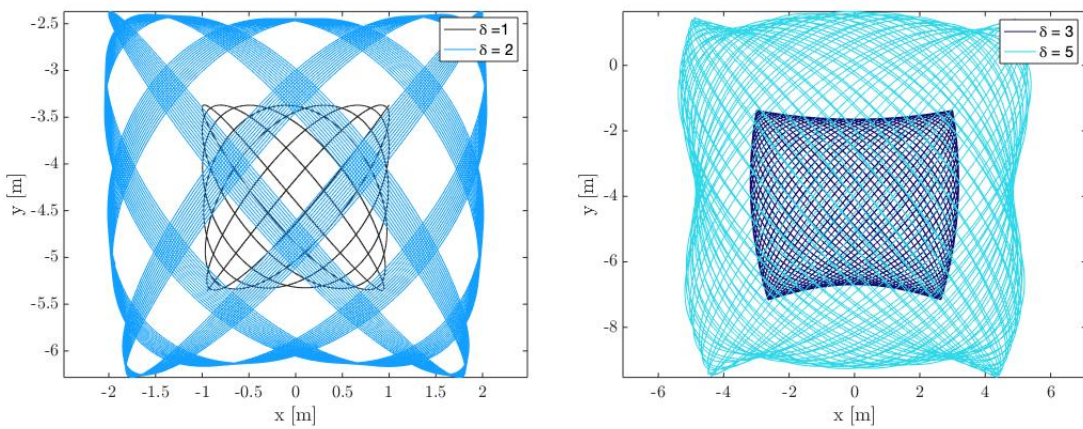


Figure (13) Trajectory of the pendulum with initial positions :  $(x_0, y_0) = (x_{eq} + \delta, y_{eq} + \delta)$

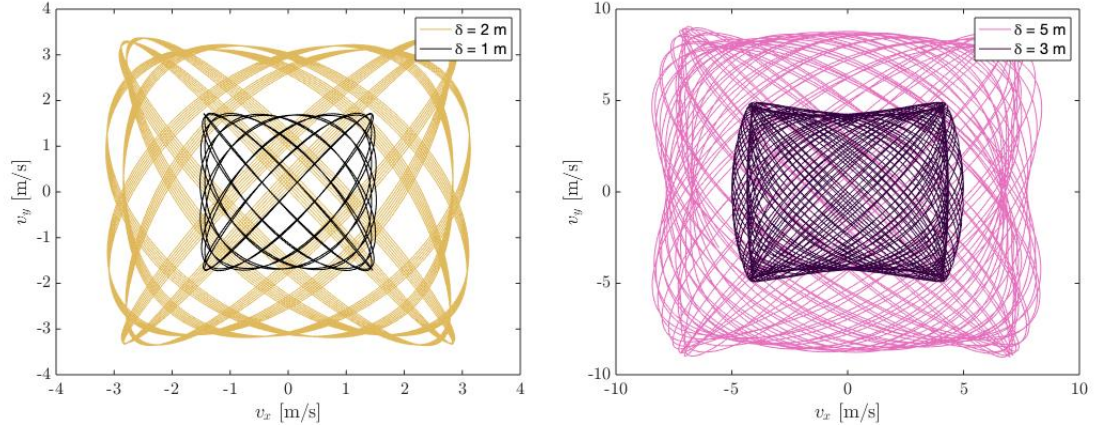


Figure (14) Pendulum speed with initial positions :  $(x_0, y_0) = (x_{eq} + \delta, y_{eq} + \delta)$

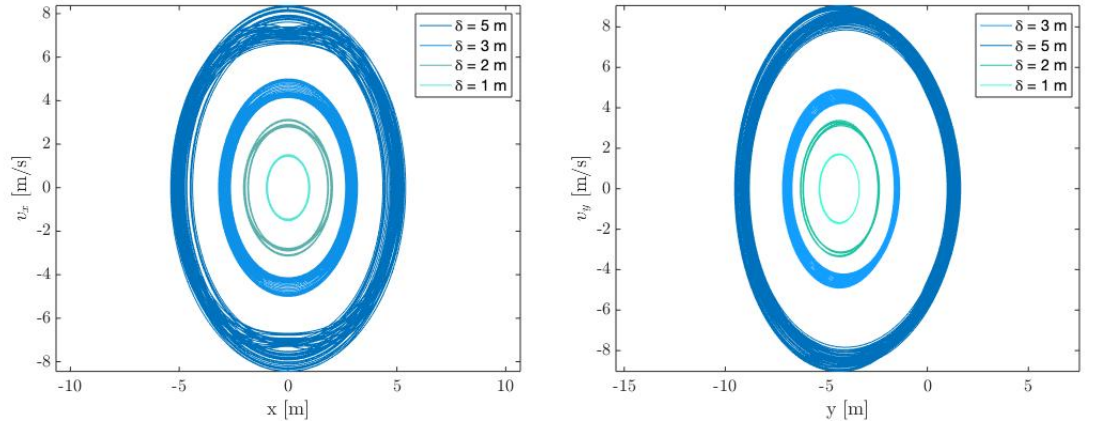


Figure (15) Orbits in the plane  $(x, v_x)$  left side, orbits in the plane  $(y, v_y)$  right side, at initial position  $(x_0, y_0) = (x_{eq} + \delta, y_{eq} + \delta)$

### 3.3.2 Study on the conservation of $E_{mec}$ when $\delta = 3$ and convergence rate

As regards to the mechanical energy of the system, represented as a function of the time at Fig. 16, we notice that it is preserved. Indeed, the value of  $E_{mec}$  oscillates constantly around the same value over time.

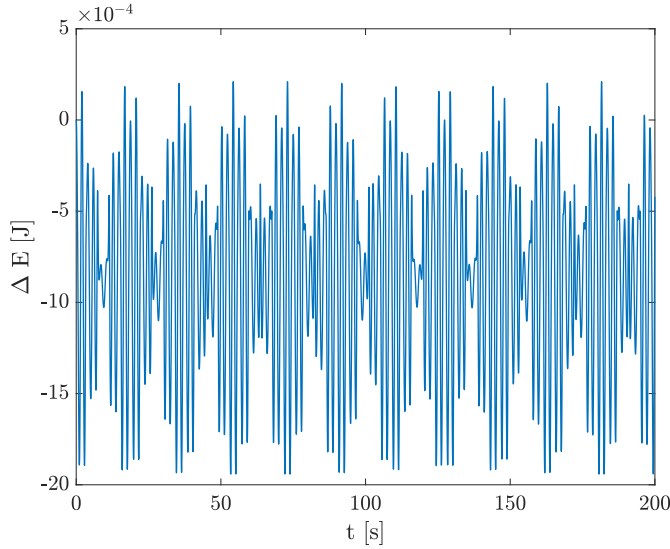


Figure (16) Mechanical energy of the pendulum depending on time, at initial positions  $x_0, y_0 = 3, -1.37$

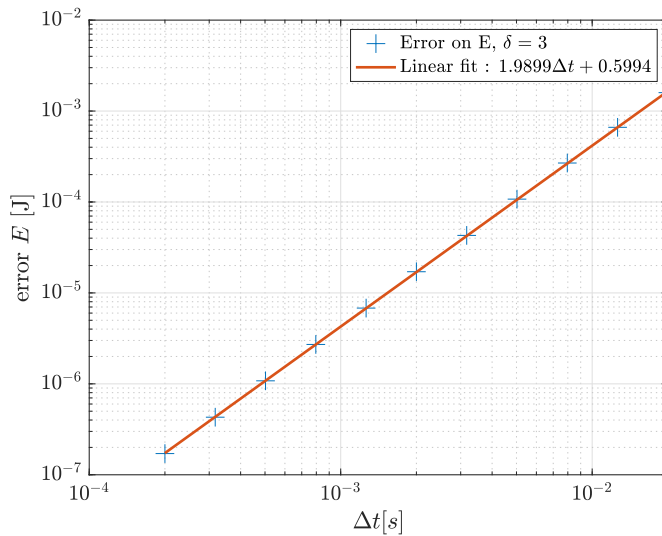


Figure (17) Convergence rate of the Verlet scheme for 11 simulations with a log-log scale with the fitting curve

In this case, the analytical solution for  $E_{mec}$  at the initial time is known,  $E_{mec} \simeq -9,29\text{J}$ . So it is possible to compute  $Error_{E_{mec}} = E_{mecAnalytical} - E_{mecNumerical}$ .

In Fig.17 which represents the error as a function of  $\Delta t$  with a log-log scale, the slope represents the convergence rate. Hence its converges order 2.

### 3.4 Big movement without depreciation, with excitation

In this subsection, the movement of the pendulum is analysed. An oblique electric field ( $E_x = E_y = 5 \times 10^{-3} \text{ V} \cdot \text{s}^{-1}$ ) with frequency  $\omega = 1.65 \text{ s}^{-1}$  are considered. The time step  $\Delta t = \frac{T}{N}$  where  $T$  is the period and  $N$  and integer (There is  $N$  steps during one period). The initial conditions are defined later as follows:  $x_0 = x_{eq} + \delta$ ,  $y_0 = y_{eq} + \delta$  where  $\delta$  is defined later.

#### 3.4.1 Theorem of mechanical energy

In order to check if the theorem of mechanical energy ( $\frac{dE_{mec}}{dt} = P_{nc}$ ) is verified, the graph of the difference  $\frac{dE_{mec}}{dt} - P_{nc}$  as a function of the time is plotted when  $\delta = 2\text{m}$  and  $t_{final} = 200\text{m}$  (Fig 18). If the theorem was perfectly verified, this graph should be constantly equal to 0.

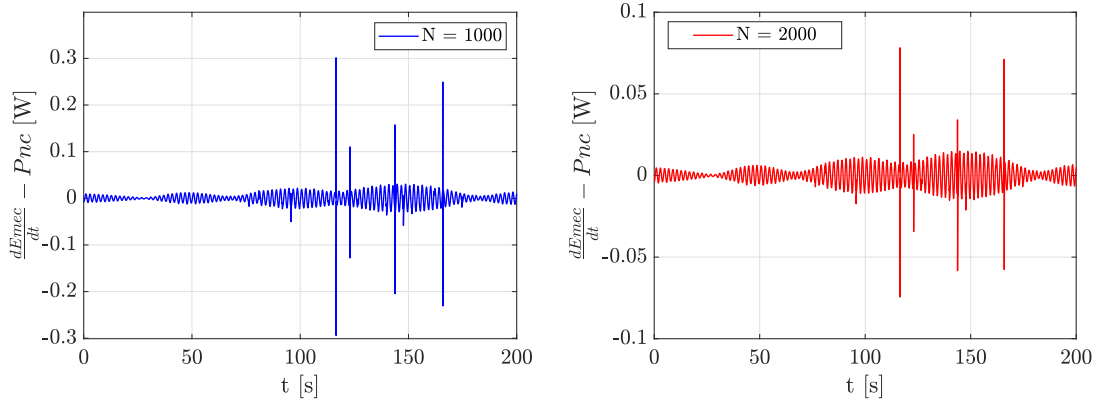


Figure (18)  $\frac{dE_{mec}}{dt} - P_{nc}$  as a function of the time for two different  $\Delta t$  Left:  $N = 1000$ . Right:  $N = 20000$

It is possible to see that the theorem is globally verified. Indeed, the difference oscillates around 0 and the error is very small. As it is possible to see on Fig 18, a way to decrease the error is to decrease  $\Delta t$  by increasing  $N$ . The peaks are due to numerical errors. Indeed, we can see that it decreases enormously if  $\Delta t$  is decreased.

### 3.4.2 Poincaré section

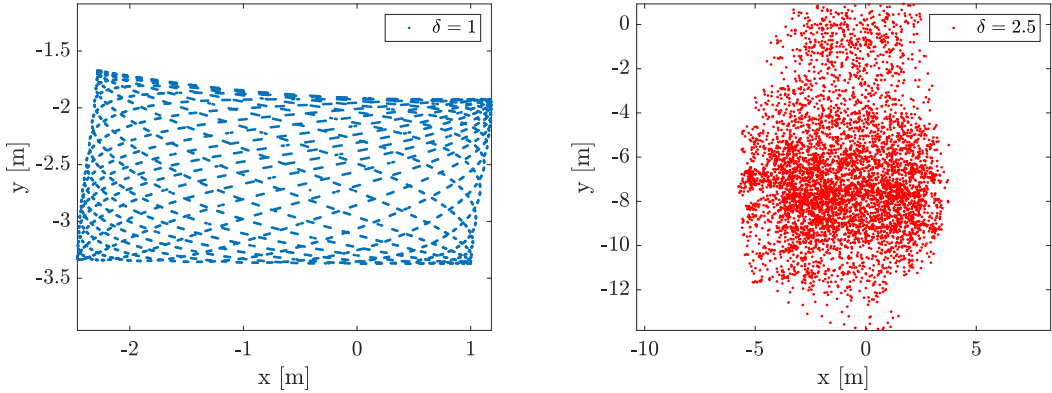


Figure (19) Poincaré section of the space phase ( $x, y$ ). Left:  $\delta = 1$ . Right:  $\delta = 2.5$

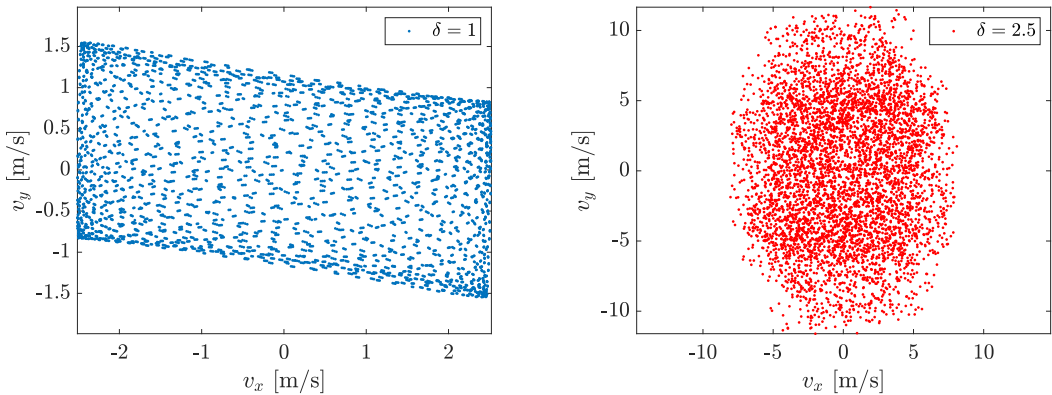


Figure (20) Poincaré section of the space phase ( $v_x, v_y$ ). Left:  $\delta = 1$ . Right:  $\delta = 2.5$

A Poincaré section is an output which contains only one point per period. That means that we represent a projection in a plane of the phase space of the every period of excitement. To do that, a very long simulation has to be done ( $t_{final} = 20000\text{s}$ ) with 1000 time steps per period ( $N = 1000$ ) and  $sampling = 1000$  ( $N = sampling$ ). In this case, the Poincaré section are used to analyse the phase space of  $(x, y)$ ,  $(x, v_x)$ ,  $(y, v_y)$ ,  $(v_x, v_y)$ .

Here, the Poincaré section for  $\delta = 1\text{m}$  and  $\delta = 2.5$  are compared in Fig 19, 20 and 21 . It is obvious to see that these two behaves completely differently:

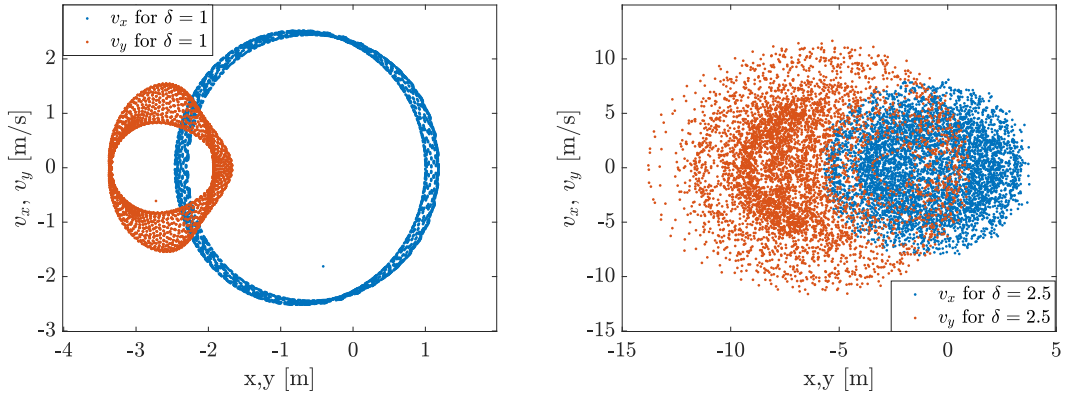


Figure (21) Poincaré section of the space phases  $(x, v_x)$  and  $(y, v_y)$ . Left:  $\delta = 1$ . Right:  $\delta = 2.5$

Fig 22 shows that when  $\delta$  is smaller than a certain value, the space phases are very clean. But when  $\delta$  is bigger than this value (Fig 23), the space phases are more and more chaotic. Here, this value is between 1.48m and 1.49m.

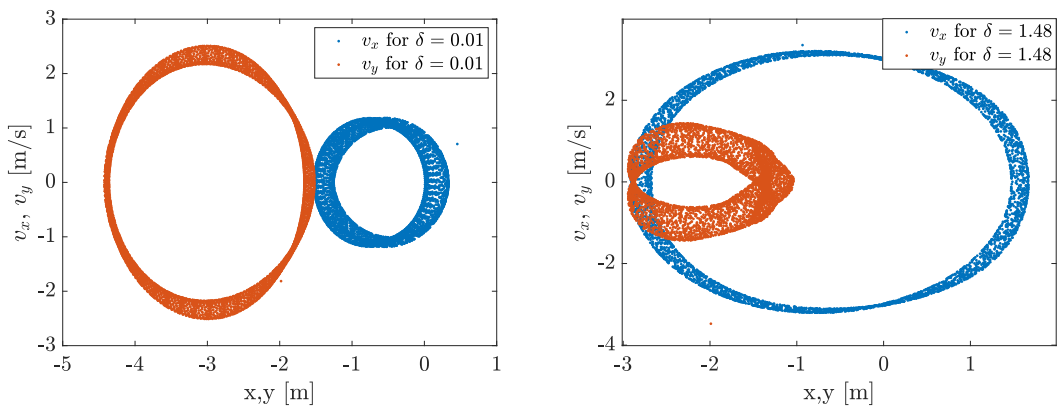


Figure (22) Poincaré section of the space phases  $(x, v_x)$  and  $(y, v_y)$ . Left:  $\delta = 0.01$ . Right:  $\delta = 1.48$

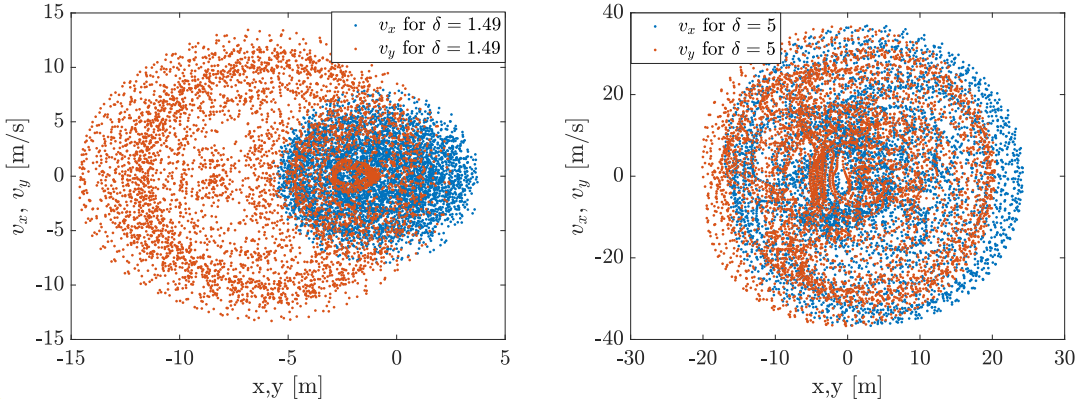


Figure (23) Poincaré section of the space phases  $(x, v_x)$  and  $(y, v_y)$ . Left:  $\delta = 1.49$ . Right:  $\delta = 5$

### 3.4.3 Sensitivity to initial conditions

Here, the sensitivity of pendulum to the initial conditions are analysed by the Poincaré sections.

First, two simulations with final time  $t_{final} = 800$ s and  $sampling = 1$  are made with initial conditions close to  $10^{-9}$ m and the distance  $d$  between the two orbit is plotted as a function of the time. Where  $d$  is calculate by:

$$d(t) = \sqrt{(\mathbf{x}_1(t) - \mathbf{x}_2(t))^2 + (\mathbf{v}_1(t) - \mathbf{v}_2(t))^2 / \omega^2} \quad (23)$$

$\mathbf{v}_i(t)$  and  $\mathbf{x}_i(t)$  represent the velocity and the position of the pendulum i at time t.

Fig. 24 and 28 represent the distance between the orbits given by  $(x_1, y_1) = (x_{eq} + \delta, y_{eq} + \delta)$  and  $(x_2, y_2) = (x_{eq} + \delta + 10^{-9}, y_{eq} + \delta)$  where  $\delta = 1$  and  $\delta = 2.5$  respectively. A semi-log scale is used to highlight the exponential divergence  $d(t)$ . In the case  $\delta = 1$ , it is possible to see on Fig. 24 that  $d(t)$  converges exponentially to a very small value of  $\approx 10^{-8}$ m. That means that in this case, there is fast no difference between the two orbits. Indeed if we superpose the Poincaré sections for  $\delta = 1$  and for  $\delta = 1$  with a perturbation of  $10^{-9}$  on x (25), they are hardly the same. Because when we superpose them, it is impossible to differentiate them. But if a big zoom is made (27), it is possible to see a very small difference between them. Results are similar for the Poincaré sections of the phases  $(x, v_x)$  and  $(y, v_y)$  (Fig. 26).

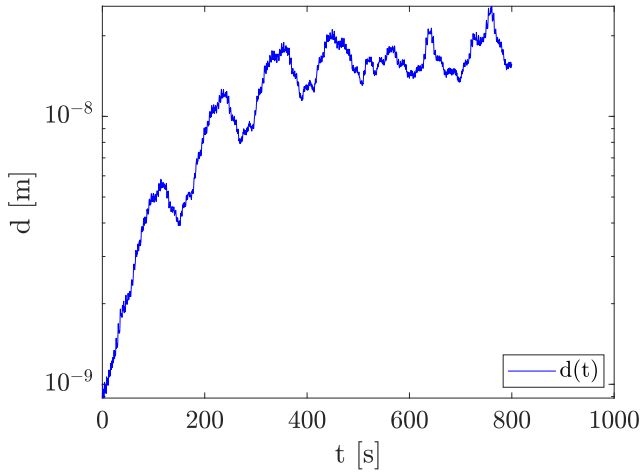


Figure (24) Distance between the two orbits given by  $(x_1, y_1) = (1, -3.37)$  ( $\delta = 1$ ) and  $(x_2, y_2) = (1 + 10^{-9}, -3.37)$ .

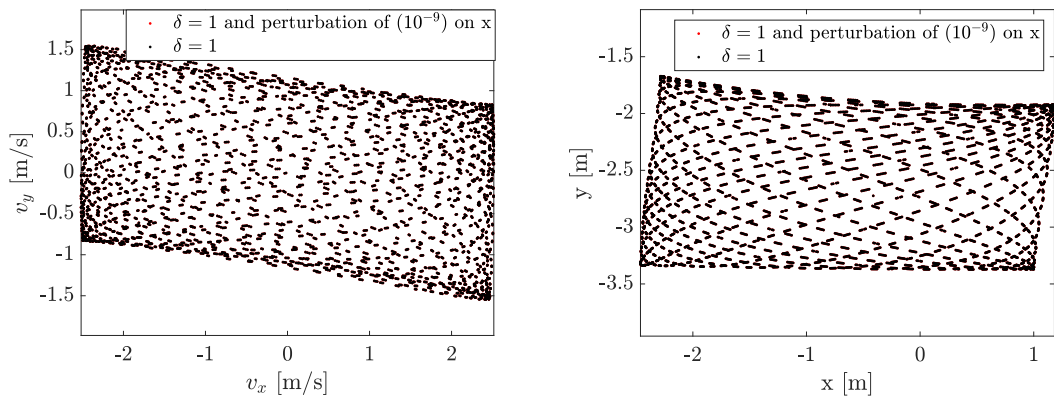


Figure (25) Superposition of two Poincaré section. Left: Poincaré section of the space phases  $(v_x, v_y)$ , Right: Poincaré section of the space phases  $(x, y)$

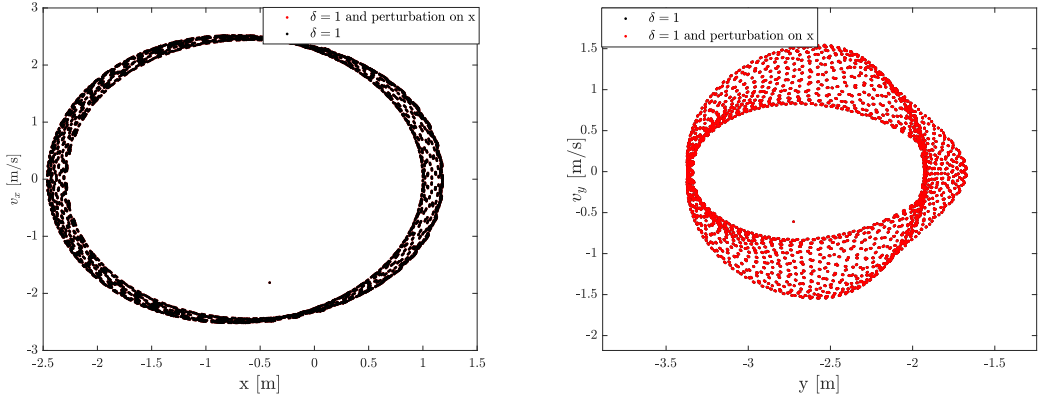


Figure (26) Superposition of two Poincaré section. Left: Poincaré section of the space phases  $(x, v_x)$ , Right: Poincaré section of the space phases  $(y, v_y)$

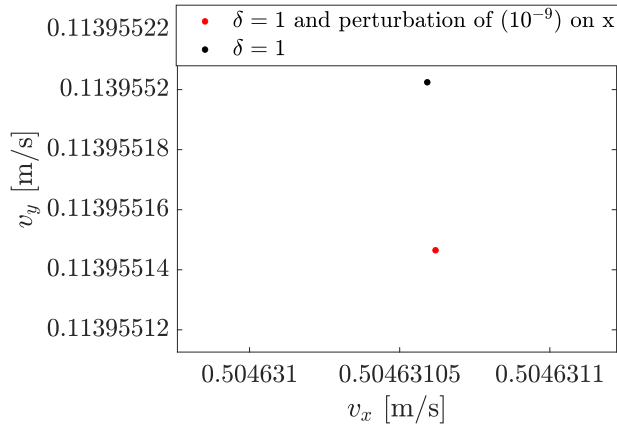


Figure (27) Big zoom on a random point of Fig 25(left)

In the case  $\delta = 2.5$ , it is possible to see on Fig. 28 that  $d(t)$  converges exponentially, but to a bigger value than before. That means that the distance between the orbit is bigger than in the case  $\delta = 1$ . Indeed, the superposition of the Poincaré section of  $\delta = 2.5$  and  $\delta = 2.5$  with a little perturbation are not the same (Fig 29). Results are similar for the Poincaré sections of the phases  $(x, v_x)$  and  $(y, v_y)$  (Fig. 30).

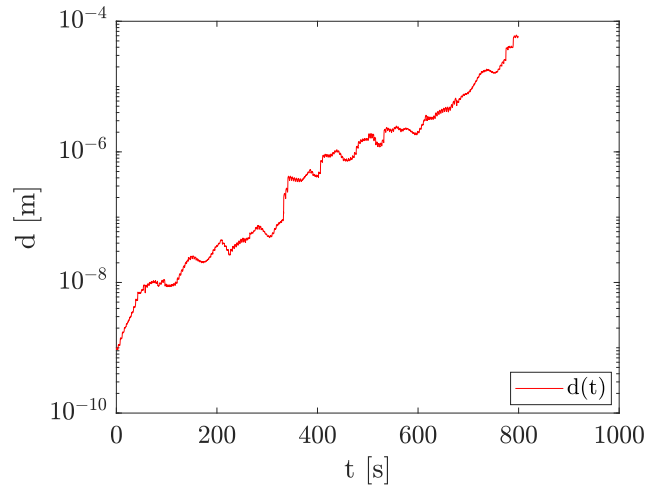


Figure (28) Distance between the two orbits given by  $(x_1, y_1) = (2.5, -1.87)$  ( $\delta = 2.5$ ) and  $(x_2, y_2) = (2.5 + 10^{-9}, -1.87)$ .

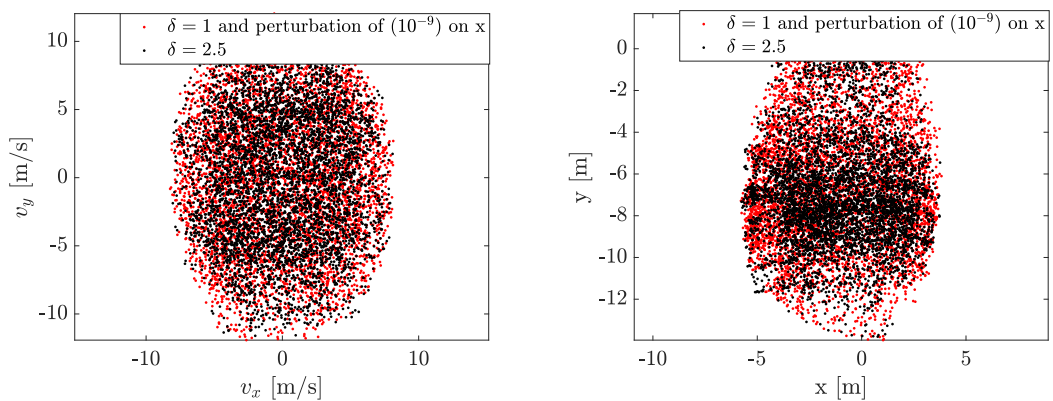


Figure (29) Superposition of two Poincaré section. Left: Poincaré section of the space phases  $(v_x, v_y)$ , Right: Poincaré section of the space phases  $(x, y)$

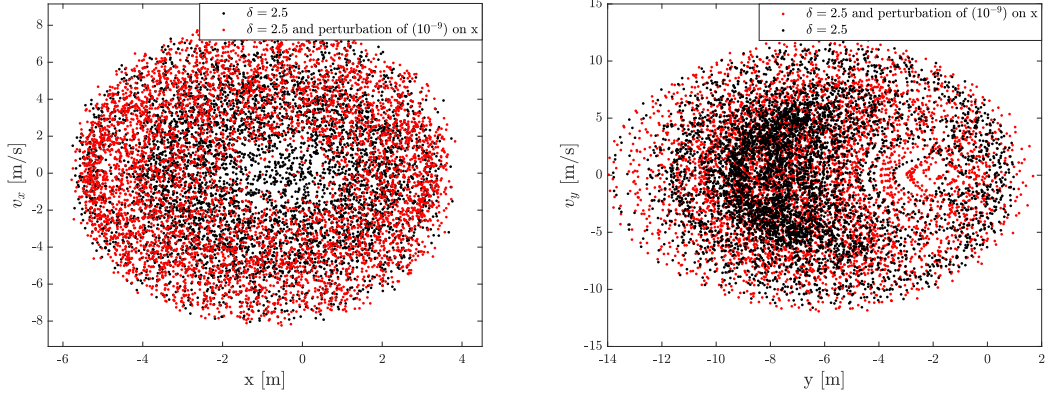


Figure (30) Superposition of two Poincaré section. Left: Poincaré section of the space phases  $(x, v_x)$ , Right: Poincaré section of the space phases  $(y, v_y)$

### 3.5 Big movement with damping and with excitation

In this section, one is considering a depreciation  $\nu = 0.01 \text{kg} \cdot \text{s}^{-1}$  and an excitation with an oblique electrical field :  $E_x = E_y = 5 \times 10^{-3} \text{V} \cdot \text{s}^{-1}$  with  $\omega_1$  as frequency. For the simulations  $N = 1000$  and  $\Delta t = \frac{T}{N} \simeq 3.63 \times 10^{-3} \text{s}$ . The goal is to study chaos and strange attractor.

#### 3.5.1 Verification of the Mechanical Energy Theorem

In this subsection, the goal is to verify the  $E_{\text{Mec}}$  theorem as in 3.4.1. Here  $\delta = 2.5$  and the final time taken is  $t_f = 200$ s. In order to verify this theorem two different figure were studied. The first one Fig.31 represents the relative error of the difference between  $\frac{dE_{\text{mec}}}{dt}$  and  $P_{\text{nc}}$ . One can see that there are some spikes and so we are not sure that the theorem is verified. Fig.32 represents  $P_{\text{nc}}$  and  $\frac{dE_{\text{mec}}}{dt}$  as a function of time. One can notice that it is difficult to distinguish the two curves. The presence of the spikes on Fig.31 can be explained. Indeed, one can see that the biggest spike appears at  $\approx 105$ s on Fig.31. Looking at Fig.32 one see that at 105s the value of  $P_{\text{nc}}$  is close to zero. Therefore these spikes come from the calculation of relative error. When  $P_{\text{nc}}$  is close to zero  $(\frac{dE_{\text{mec}}}{dt} - P_{\text{nc}})/P_{\text{nc}}$  will towards big values. Hence, the theorem of  $E_{\text{mec}}$  is verified.

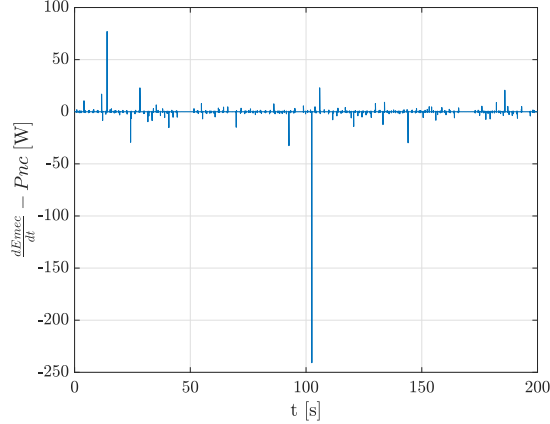


Figure (31) Difference between the mechanical energy and power of the non-conservative forces as a function of time, at initial position  $(x_0, y_0) = (2.5, -1.87)$

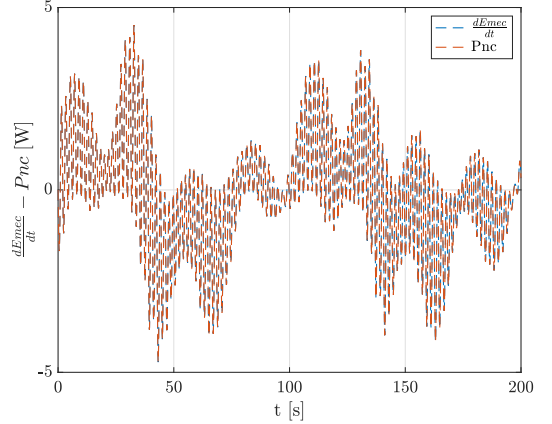


Figure (32) Respectively the mechanical energy and the power of the non-conservative forces as a function of time, at initial position  $(x_0, y_0) = (2.5, -1.87)$

### 3.5.2 Signature of chaos : sensitivity to initial condition

Here (like in section 3.4.3), two simulations with initial positions distant from  $10^{-9}\text{m}$  are done the initial position taken are :  $(x_1, y_1) = (2.5, -1.87)$  ( $\delta = 2.5$ ) and  $(x_2, y_2) = (2.5 + 10^{-9}, -1.87)$ . The distance between two orbits is defined by eq.(23) :

As before, a semi-log scale is used to highlight the exponential divergence  $d(t)$ , Fig.33. Indeed one see that  $d(t)$  converges exponentially, leaving approximately of zero to reach an asymptotic value around which it will vary. It is important to notice that, because the friction coefficient  $\nu$  is not zero, the distance between the two orbits is far bigger than in section 3.4.3 (where  $\nu = 0$ ). In this case, it is interesting to define the Lyapunov exponent which allows to quantify the instability of a system with very initial conditions close, but not equal. Infinitesimal uncertainty about initial conditions converges exponentially over time. It can be determined using eq.(24).

$$|\delta d(t)| \approx \exp(at) \cdot |\delta d_0| \quad (24)$$

It then represents the slope observable over the first  $\approx 575$  seconds. As it describes an unstable movement, there is an elongation and it therefore it is concluded that the system is very sensitive to the initial conditions. The

positivity of this exponent is a necessary (but not sufficient) condition for achieving instability and the chaos.

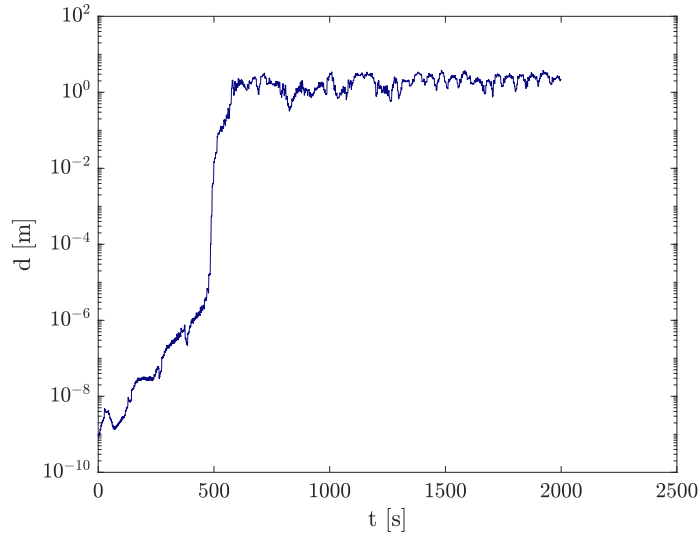


Figure (33) Distance between the two orbits given by  $(x_1, y_1) = (2.5, -1.87)$  and  $(x_2, y_2) = (2.5 + 10^{-9}, -1.87)$ .

### 3.5.3 The Poincaré section

In this subsection a long simulation is done. The final time taken is  $t_f = 20000$ s with  $N = 1000$  (time steps per period). The initial position used is  $(x_0, y_0) = (2.5, -1.87)$  ( $\delta = 2.5$ m). In opposition with the orbits in Fig.13, the trajectory of the pendulum is not regular, Fig.34 and Fig.35. This was expected because we are in a situation of chaos. Nevertheless, it still fits a defined geometrical area. One can remark that as in 3.3.1, Fig.34 and Fig.35 have the same shape. In Fig.36 and in Fig.37, one can look at the orbit in the plane  $(x, v_x)$  and  $(y, v_y)$ .

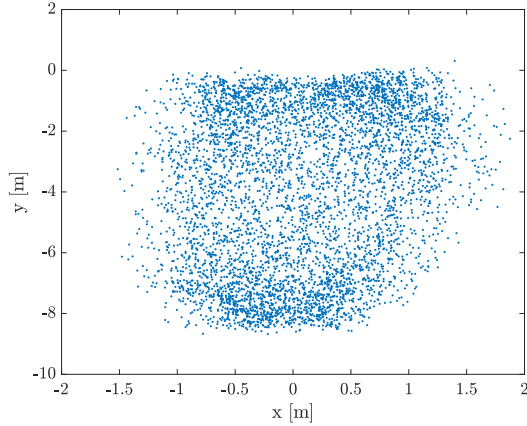


Figure (34) Orbit in the plane  $(x, y)$

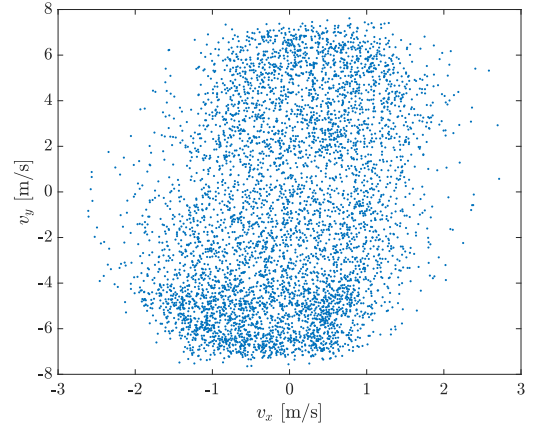


Figure (35) Orbit in the plane  $(v_x, v_y)$

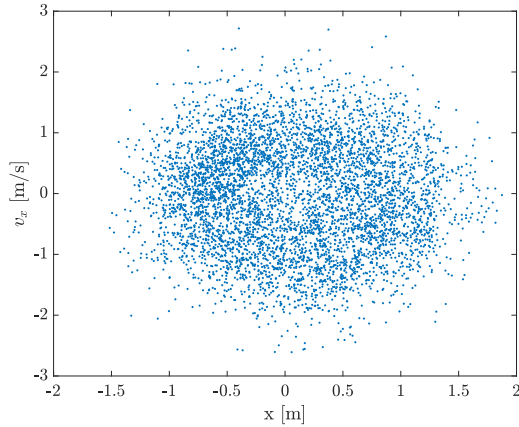


Figure (36) Orbits in the plane  $(x, v_x)$

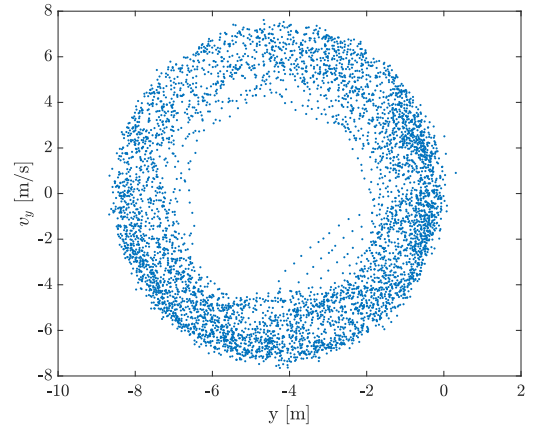


Figure (37) Orbits in the plane  $(y, v_y)$

It is interesting to see that the Fig.37 still represents an ellipse pretty well defined. This means that the vertical pendulum motion is still an harmonic motion. This is not the case for the horizontal motion. To illustrate this comment one can look at the Fig.38 which shows that respectively  $y$  and  $v_y$  as a function of  $t$  have approximately the shape of a sinusoidal.

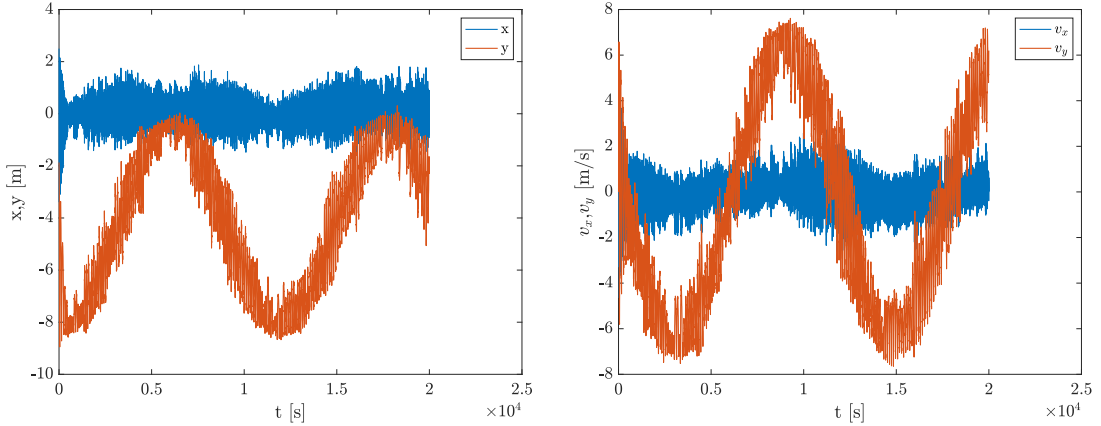


Figure (38) Respectively  $(x, y)$  and  $(v_x, v_y)$  as a function of  $t$ , at initial position  $(x_0, y_0) = (2.5, -1.87)$

### 3.5.4 Strange attractor

The purpose of this section is to demonstrate that either the initial position imposed on our system the attractor of our diagram of phase will remain substantially identical. For this, three different initial position where taken by varying  $\delta = 1.5, 2.5$  and  $3.5$  m. In order to compare the diagram according to the initial position, the diagrams have been superposed Fig.39. Through Fig.39, we can then see that the values obtained during simulations are not exactly identical but have a tendency to be located in the same area. This represents the presence of an attractor in the phase diagram as one can see Fig.39. Its attractor name comes from the fact that it "attracts" any initial condition whatever its value.

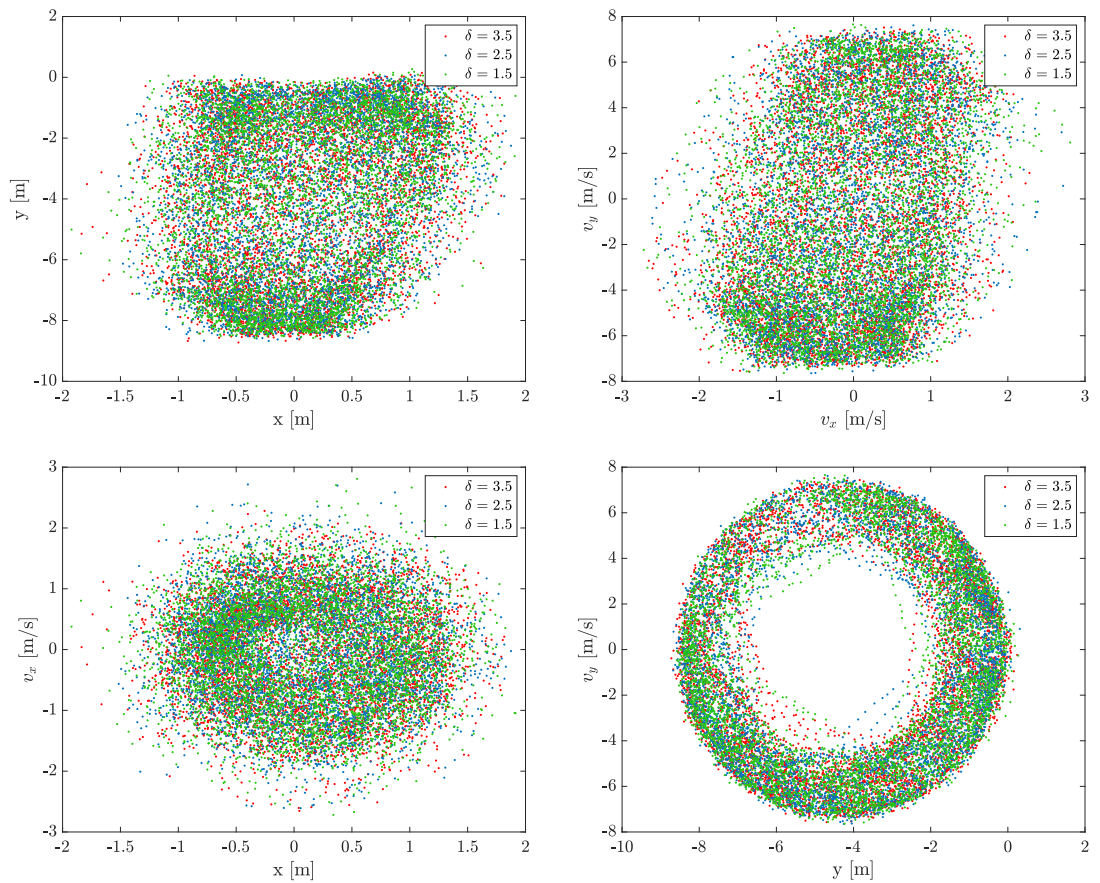


Figure (39) Superposition of orbits in 4 different planes at initial position  $x_0 = x_{eq} + \delta$  and  $y_0 = y_{eq} + \delta$ , with  $\delta = 1.5, 2.5$  and  $3.5\text{m}$

## 4 Optional

### 4.1 Inclusion of an oscillating force resulting from the application of torque

In this section, an oscillating force,  $\mathbf{F}_c = \left(\frac{c}{l}\right) \sin(\omega t) \mathbf{e}_\theta$ , resulting from the application of a torque with a given torque is added to the system.  $c$  is the torque (Nm). In the cartesian coordinates, the projection of this force on the x-axis and y-axis is:

$$\mathbf{F}_c = \frac{c}{x^2 + y^2} \sin \omega t \cdot (-y \mathbf{e}_x + x \mathbf{e}_y) \quad (25)$$

In the case of Fig. 40 and Fig. 41, simulations are made with final time  $t_{final} = 20000$ s, no friction coefficient and no excitation ( $\mathbf{E} = 0$ ). There is 1000 time steps per period and *sampling* = 1000 in order to have Poincaré sections.

As in Section 3.5.4, it can be noted that the Poincaré sections are similar regardless of the initial conditions (Fig. 40). Indeed, the values obtained during simulations are not exactly identical but have a tendency to be located in the same area. This represents the presence of an attractor again. Note that for the plane  $(y, v_y)$  in Fig. 40, an other  $\delta$  has been chosen to show more clearly the attractor. Moreover, a big torque has been choosed because the graphs were clearer than with a small torque. It should be noted that the larger the torque, the bigger are the pendulum movement (Fig. 41)

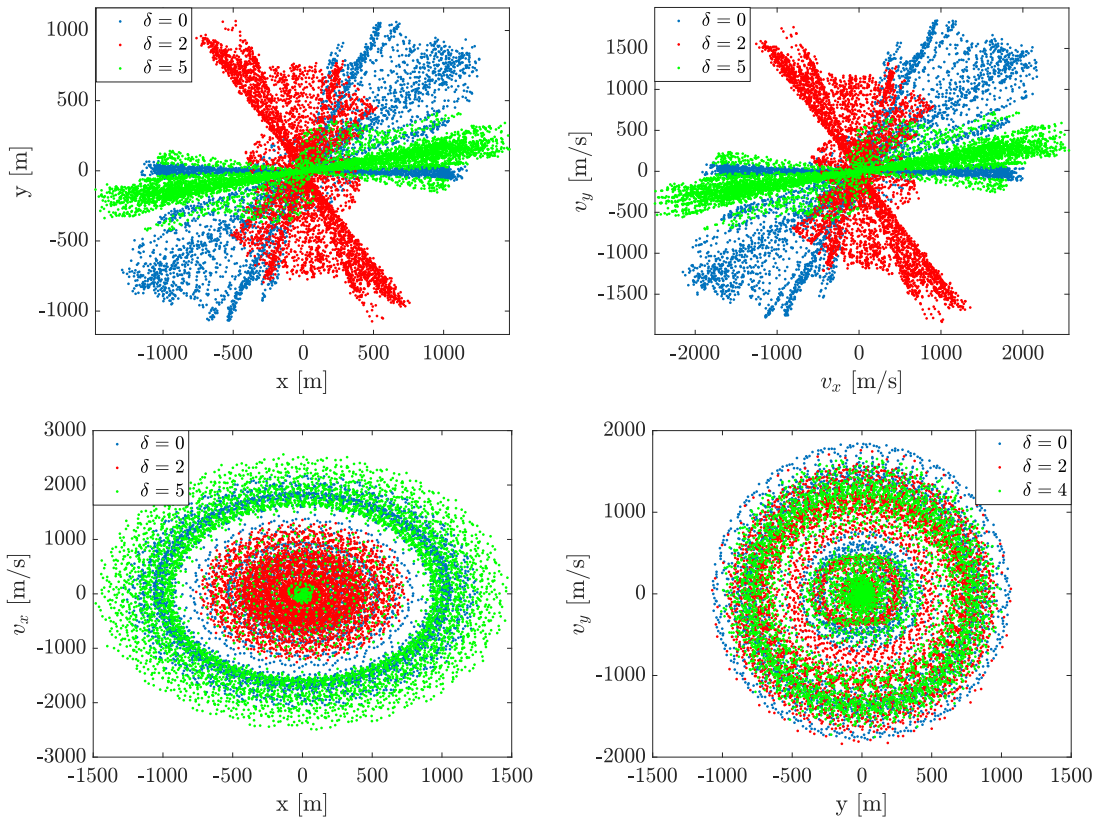


Figure (40) Superposition of orbits in 4 different planes when an oscillating force resulting from an application of a torque  $c = 10000$ . Initial position  $x_0 = x_{eq} + \delta$  and  $y_0 = y_{eq} + \delta$ , with  $\delta = 0, 2$  and  $5\text{m}$  for all the figure except for  $(y, v_y)$  where  $\delta = 0, 2$  and  $4\text{m}$ .

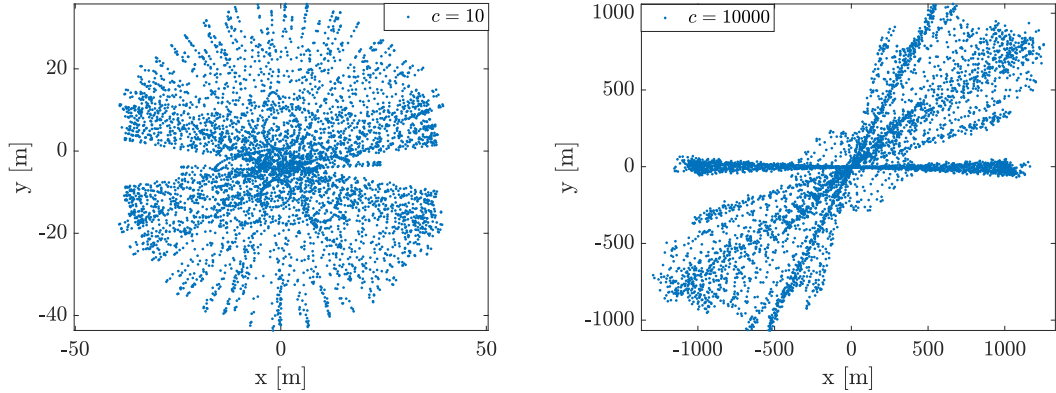


Figure (41) Pendulum movement when the torque is changed. Left:  $c = 10$ , Right:  $c = 10000$ . Initial position  $(x_0, y_0) = (x_{eq}, y_{eq})$

## 5 Conclusion

Through this study, a more precise definition of chaos has been established. One have seen that when small movements around the equilibrium position or small excitation are considered, it is still possible to predict the movement. But, as soon as frictional forces are taken into consideration the system evolves over times towards chaos whatever the initial condition. Indeed, starting at two very close position, one can see that the system evolves exponentially to two distinct position. However, the Poincaré section enables to situate the motion of the spring pendulum. Even though the system is chaotic it is not random.

## References

- [1] Physique numérique I-II Laurent Villard
- [2] [https://phys.libretexts.org/Bookshelves/University\\_Physics/Book%3A\\_University\\_Physics\\_\(OpenStax\)/Map%3A\\_University\\_Physics\\_I\\_-\\_Mechanics%2C\\_Sound%2C\\_Oscillations%2C\\_and\\_Waves\\_\(OpenStax\)/8%3A\\_Potential\\_Energy\\_and\\_Conservation\\_of\\_Energy/8.2%3A\\_Conservative\\_and\\_Non-Conervative\\_Forces#targetText=Non-conservative%20forces%20are%20dissipative,the%20object%20starts%20and%20stops.](https://phys.libretexts.org/Bookshelves/University_Physics/Book%3A_University_Physics_(OpenStax)/Map%3A_University_Physics_I_-_Mechanics%2C_Sound%2C_Oscillations%2C_and_Waves_(OpenStax)/8%3A_Potential_Energy_and_Conservation_of_Energy/8.2%3A_Conservative_and_Non-Conervative_Forces#targetText=Non-conservative%20forces%20are%20dissipative,the%20object%20starts%20and%20stops.)